

Mechanical wet-milling and subsequent consolidation of ultra-fine Al_2O_3 -(ZrO_2 +3% Y_2O_3) bioceramics by using high-frequency induction heat sintering

Khalil Abdelrazek KHALIL, Sug Won KIM

Division of Advanced Materials Engineering, RIAMD, Chonbuk National University,
Jeonju 561-756, South Korea

Received 17 March 2006, accepted 13 September 2006

Abstract: Alumina/zirconia composites were synthesized by wet-milling technique and rapid consolidation with high frequency induction heat sintering(HFIHS). The starting materials were a mixture of alumina micro-powder (80%, volume fraction) and 3YSZ nano-powders (20%). The mixtures were optimized for good sintering behaviors and mechanical properties. Nano-crystalline grains are obtained after 24 h milling. The nano-structured powder compacts are then processed to full density at different temperatures by HFIHS. Effects of temperature on the mechanical and microstructure properties were studied. Al_2O_3 -3YSZ composites with higher mechanical properties and small grain size are successfully developed at relatively low temperatures through this technique.

Key words: bioceramic; alumina; zirconia, mechanical wet-milling, sintering

1 Introduction

Due to biocompatibility and their high mechanical properties, alumina-zirconia composites are one of the relatively good and promising candidates for biomaterials that combine high flexural strength with high toughness[1–6]. The mechanical properties of nanoceramics such as hardness and strength are generally superior to those of conventional ceramics[7–9]. One of the main impediments to the use of nanostarter powders is their higher cost and the retainment of the nanostructure in the final product after exposure to elevated temperatures during conventional methods of powder consolidation[10]. It is therefore essential to minimize grain growth through careful control of consolidation parameters, particularly sintering temperature and time. The novel technique of HFIHS has been shown to be an effective sintering method that can successfully consolidate ceramics and metallic powders to near theoretical density[11–14]. The novel HFIHS process is a sintering method for the rapid sintering of nanostructured hard metals in a very short time of

high-temperature exposure with pressure application. It is similar to hot pressing, which is carried out in a graphite die, but the heating is accomplished by a source of high frequency electricity to drive a large alternating current through a coil. This coil is known as the work coil. The passage of current through this coil generates a very intense and rapidly changing magnetic field in the space within the work coil. The workpiece to be heated is placed within this intense alternating magnetic field. The alternating magnetic field induces a current flow in the conductive workpiece. Induction heating has many advantages over competing techniques, such as radiancy or convection heat and laser technologies. Since it is non-contact, and the heat is transferred to the product via electromagnetic waves, the heating process does not contaminate the material being heated. The objective of this study was to synthesize and sinter alumina-3YSZ powders with fine grain size and homogeneous constituent distribution using HFIHS.

2 Experimental

Alumina powders (mean particle size 2.91 μm ,

purity 99.5%) and 3% (mole fraction) yttria stabilized zirconia (particle size 58–76 nm, purity 99.9%) supplied by Nanostructured & Amorphous Metals, Inc., USA, were used in this study. The initial powder mixture was composed of 80% (volume fraction) alumina and 20% (volume fraction) (3 yttria stabilized zirconia). All powders were milled in a Universal Mill with a ball-to-powder mass ratio of 30:1 and a powder-to-alcohol mass ratio of about 2:1. Milling was done in polyethylene bottles using zirconia balls and was performed at a horizontal rotation velocity of 250 r/min for 24 h. After drying the mixed powders were placed in a graphite die (outside diameter 45 mm; inside diameter 20 mm; height 40 mm) and then introduced into the high-frequency induction heat machine, as shown in Fig.1.

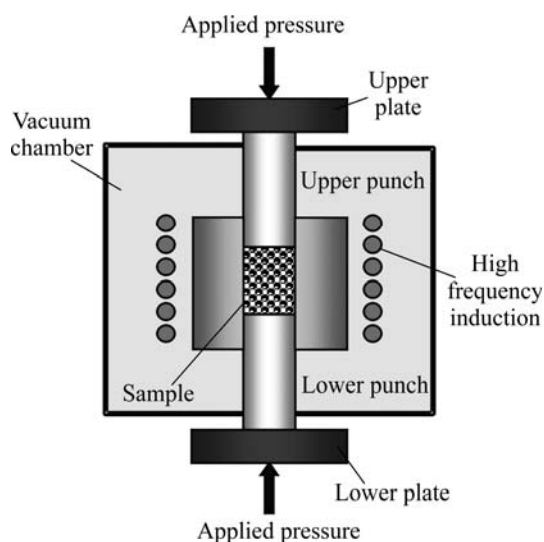


Fig.1 Schematic diagram of high-frequency induction heated sintering apparatus

The system was first evacuated to a vacuum of 37.33 Pa and a uniaxial pressure was applied. The applied pressure was measured using a strain gage based load cell with accuracy of 0.03%–0.25%. An induced current (frequency of about 50 kHz) was then activated and maintained until densification was observed. Sample shrinkage was measured by a linear gauge measuring the vertical displacement. The temperature was measured by an optical pyrometer focused on the surface of the graphite die. At the end of the process, the current was turned off and the sample was cooled to room temperature at a rate of 500 °C/min. The four stages of the HFIHS and densification process are shown in Fig.2. The density of the sintered sample was measured by the Archimedes principals and the theoretical density of the composites was measured by the rule of mixture using the theoretical density of 3.97 g/cm³ for alumina and 5.91 g/cm³ for 3YSZ. Vickers hardness and toughness

were measured by performing indentations at a load of 196 N with holding time of 15 s. Fracture toughness was given by the values of K_{IC} . The factor K_{IC} was determined using the direct crack measurement method.

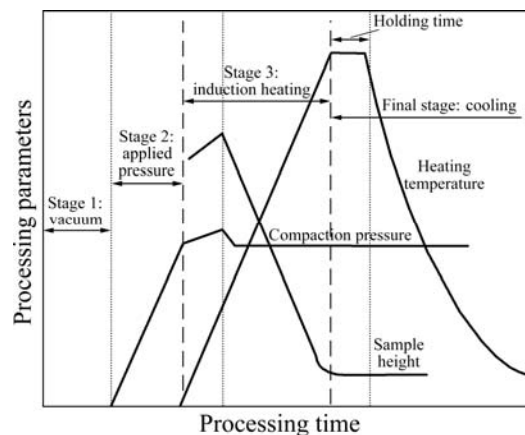


Fig.2 Four major stages of sintering process in HFIHS apparatus

3 Results and discussion

3.1 Characteristics of milled powders

Fig.3 shows morphologies of the initial Al_2O_3 powder before and after milling and the mixture of Al_2O_3 -3YSZ powder after milling for 24 h. The initial Al_2O_3 powder before milling shows multi-crystalline and agglomerations. Compared with the initial powder, the morphology of the milled powder shows more regular structures, similar to a spherical particle. Thus, the milling results in a uniform distribution of Al_2O_3 and 3YSZ powders. The refinement of grain size is resulted from the collisions between powders and balls during milling process due to increase in the kinetic energy of the ball mill. Fig.4 shows the particle size distribution of the powder. It can be seen that the powder before milling has a broad particle size distribution up to 6 μm with an average particle size of 1.156 μm (Fig.4(a)). After milling, the particle size distribution reduces for both pure alumina (Fig.4(b)) and the mixture (Fig.4(c)). The average particle size becomes 289 nm. Thus, it can be concluded that nanosized Al_2O_3 -3YSZ is prepared directly by using wet-milling technique. This technique is remarkable due to the easiness of application.

3.2 Effect of sintering temperature on shrinkage and densifications

The variations of shrinkage displacement and temperature with time at various maximum sintering temperatures under a pressure of 60 MPa are shown in Fig.5. In all cases, the application of the current and subsequent increase in the temperature result in initially thermal expansion followed by shrinkage due to con-

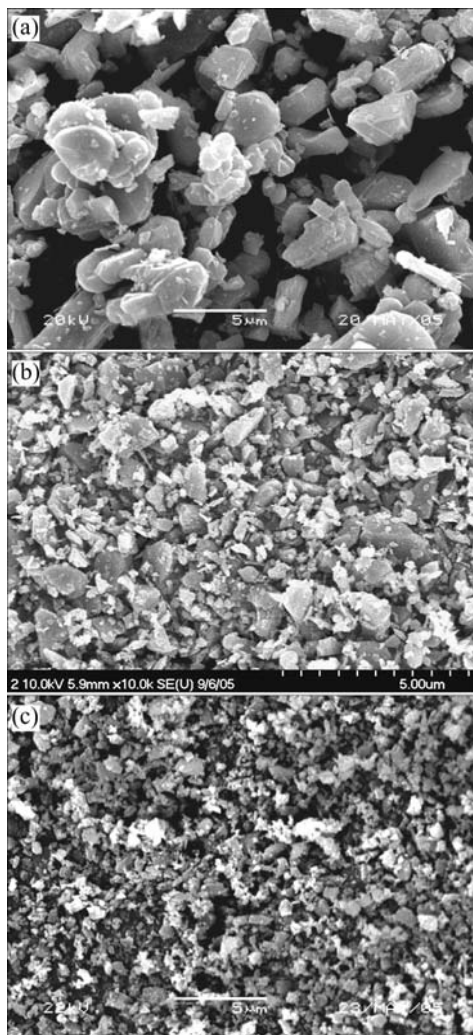


Fig.3 FE-SEM morphologies of powders: (a) Al_2O_3 powder before milling; (b) Al_2O_3 powder after milling; (c) Mixture powder after milling; (d) Mixture powder after milling with high magnification

solidation. The onset of shrinkage occurs at about 800 °C for all samples. When the temperature increases, the shrinkage displacement gradually increases. The rate of shrinkage decreases when the sintering temperature reaches the maximum. In Fig.5(b) the specimen attains maximum shrinkage before reaching the maximum sintering temperature, particularly at about 1 370 °C. Although the maximum sintering temperature reaches 1 400 °C, there is no more shrinkage after 1 370 °C. It is clear from these results that, the maximum sintering temperature with respect to maximum shrinkage is 1 370 °C. Furthermore, there is no atomic diffusion during holding time due to solid state sintering and the samples shrinkage is caused by thermo mechanical treatment. Fig.6 shows the density and relative density of Al_2O_3 -20%(volume fraction) 3YSZ as a function of sintering temperature. The relative densities of the specimens increase with increasing sintering tempera-

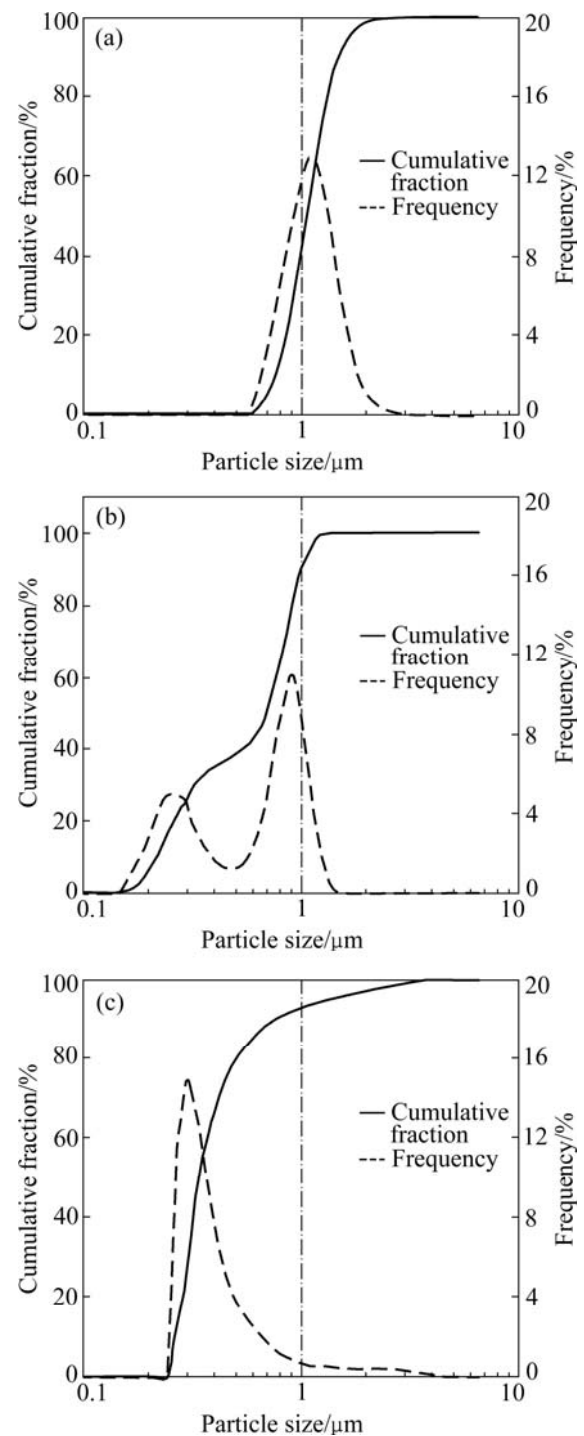


Fig.4 Particle size distribution of powders: (a) Al_2O_3 powder before milling; (b) Al_2O_3 powder after milling; (c) Mixture powder after milling

ture. It is clear that, despite the short dwelling time when the current is applied, the relative density of the sintered samples reaches as high as 99% at 1 370 °C, which means that the sintering efficiency of this method is very high. This high efficiency can be explained from two aspects. First, the high pressure applied can accelerate the densification process; second, the powder is heated

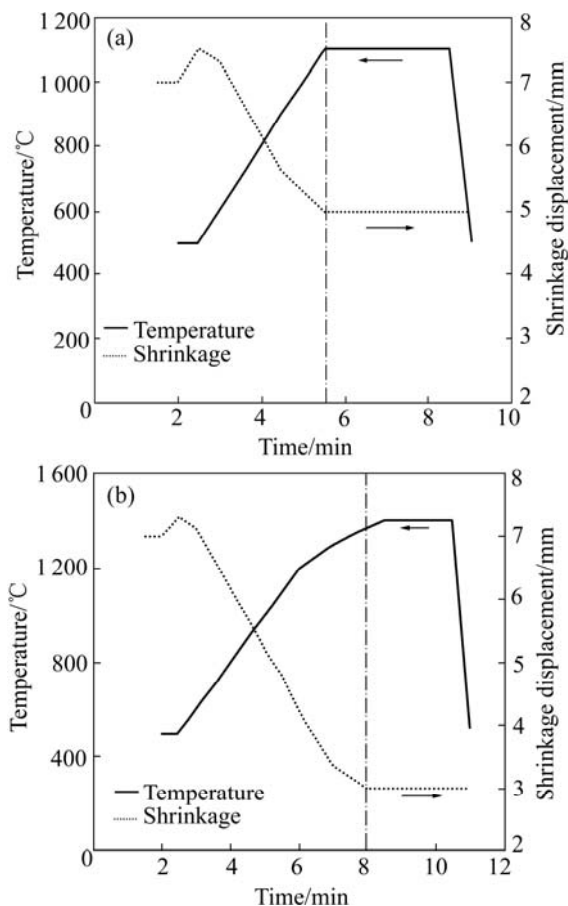


Fig.5 Variation of temperatures and shrinkage displacements vs heating time at various maximum sintering temperature: (a) 1100 °C; (b) 1400 °C

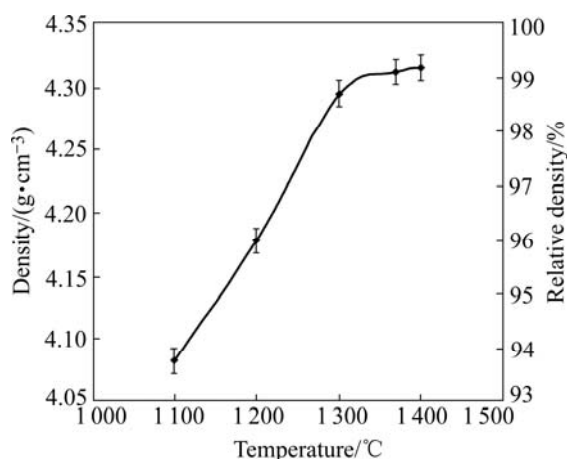


Fig.6 Density and relative density of sample vs sintering temperatures

by a very short time of high-temperature exposure. The results prove that HFIHS is a potential method for fabricating nanoceramic composites at much lower temperature and within extreme short time.

3.3 Effect of sintering temperature on hardness and fracture toughness

Vickers impressions were carried through the

surfaces of each one of the samples. The values of the Vickers hardness (GPa) were calculated by the following equation:

$$HV = 0.0018544 \left(\frac{F}{d^2} \right) \quad (1)$$

where HV is the Vickers hardness, GPa; F is the applied load, N; d is the arithmetic mean of the two diagonal length, mm. Each Vickers impression presents two pairs of radial cracks emerging from the corners.

The equation used to determine the K_{IC} values is as follows[15]:

$$K_{IC} = 0.016 \left(\frac{E}{H} \right)^{1/2} \frac{P}{C^{3/2}} \quad (2)$$

where K_{IC} is the fracture toughness; p is the applied load; E is the elastic modulus; H is the hardness; and C is the diagonal crack length. The elastic modulus was obtained by rule of mixtures starting from 380 GPa for alumina and 210 GPa for zirconia[16–18]. Fig.7 shows the relationship between Vickers hardness and fracture toughness of the Al_2O_3 -3YSZ composites as a function of sintering temperature. As expected, the Vickers hardness increases with increasing temperature, and reaches maximum at 1370 °C; while at 1400 °C, the hardness slightly decreases. This is probably caused by the influence of grain size on the hardness of the sintered composite, that is, coarser grain sizes lead to lower hardness[19–20]. The fracture toughness does not almost vary with the sintering temperature, being on the same level of approximately $5.08 \text{ MPa} \cdot \text{m}^{1/2}$.

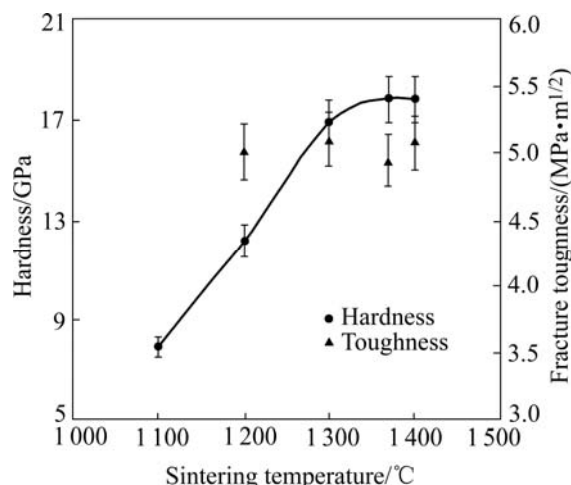


Fig.7 Hardness and toughness of sample vs sintering temperature

3.4 Effect of sintering temperature on microstructure

Fig.8 shows various SEM micrographs of the Al_2O_3 +20%(volume fraction) 3YSZ samples fracture surfaces. The microstructure seems to be like a green

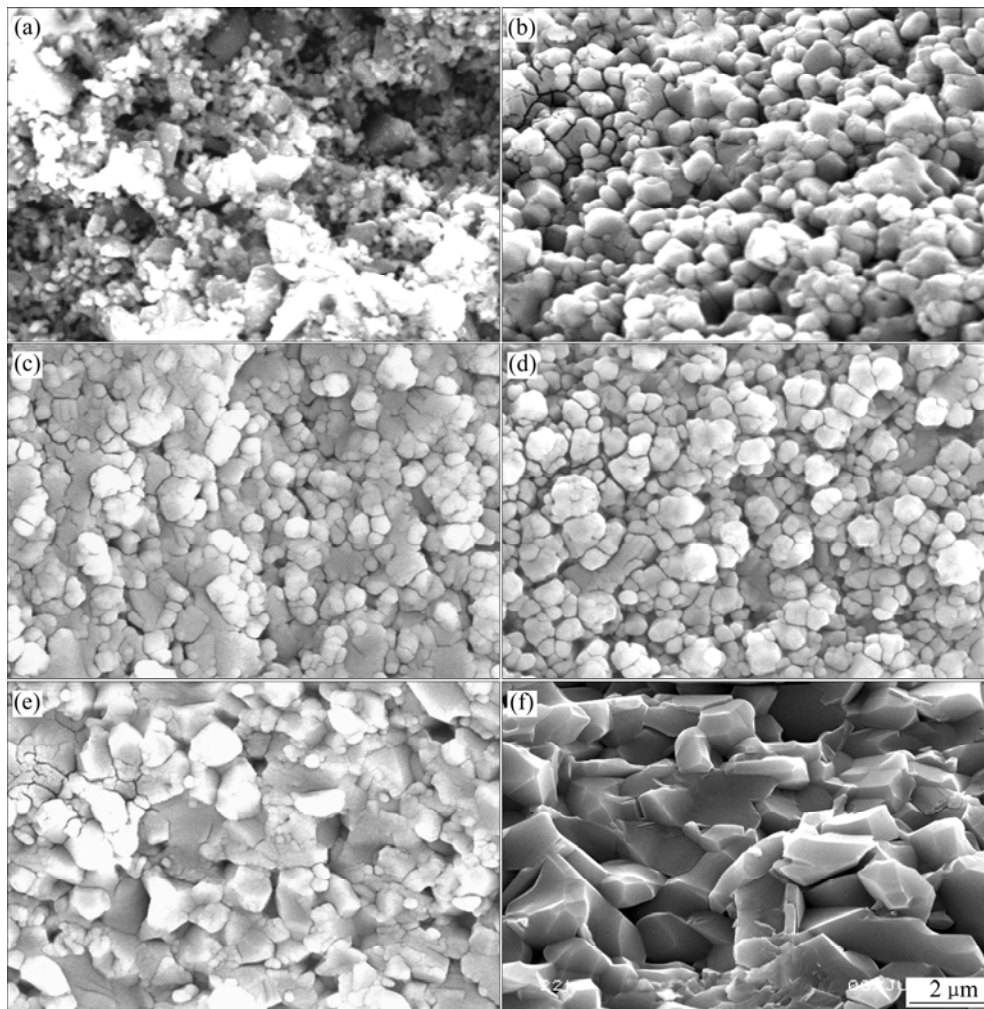


Fig.8 Effect of sintering temperature on microstructure: (a) 1 100 °C; (b) 1 200 °C; (c) 1 300 °C; (d) 1 370 °C; (e) 1 400 °C; (f) 1 400 °C (without milling)

compact for the sample sintered at 1 100 °C because the sintering temperature is low and not enough for sintering. Samples sintered at temperatures from 1 300 °C to 1 370 °C, show highly homogeneous microstructures without agglomeration, providing better densification, less porosity and no abnormally grown grains. At temperature of 1 400 °C, the grain size slightly increases with increasing temperature. For comparison the SEM fracture surface of the initial Al_2O_3 powder compacts without milling sintered at 1 400 °C is shown in Fig.8(f). It is clear that the microstructure is inhomogeneous with coarser grain size and the average grain size is about 3 μm . It can be seen that, the grain size at all sintering temperatures of the milled mixture is much smaller than that of initial alumina compact.

4 Conclusions

1) The mixtures of alumina micro-powder and 3YSZ nano- powders were synthesized and optimized by

using low energy wet-milling technique. This technique is remarkable due to the easiness of application. The mean particle size is decreased by wet-milling after 24 h of milling. After milling, the samples are superfast consolidated through the technique of high-frequency induction heated sintering (HFIHS).

2) Al_2O_3 -3YSZ composites with small grain size, homogeneous microstructure, higher density, good toughness and hardness are successfully developed at relatively low temperatures through this technique.

References

- [1] MARTI A. Inert bioceramics (Al_2O_3 , ZrO_2) for medical application, [J]. Injury Int J Care Injured, 2000(S4): 33–36.
- [2] de MORAES M C B, ELIAS C N. Mechanical properties of alumina-zirconia composites for ceramic abutments [J]. Materials Research, 2004, 7(4): 643–649.
- [3] TEKELI S, ERDOGAN M, AKTAS B. Influence of α - Al_2O_3 addition on sintering and grain growth behavior of 8mol% Y_2O_3 -stabilized cubic zirconia (c- ZrO_2) [J]. Ceramic International, 2004, 30: 2203–2209.

- [4] CHOI R, BANSAL N P. Mechanical behavior of zirconia/alumina composites [J]. *Ceramic International*, 2005, 31: 39–46.
- [5] BASU D, SARKAR B K. Effect of zirconia addition on the fatigue behavior of fine grained alumina [J]. *Bulletin of Material Science*, 2001, 24(2): 101–104.
- [6] FERNANDEZ C, VERNE E. Optimization of the synthesis of glass-ceramic matrix biocomposites by the “response surface methodology” [J]. *Journal of European Ceramic Society*, 2003, 23: 1031–1038.
- [7] MORSI K, KESHAVAN H, BAL S. Hot pressing of graded ultrafine-grained alumina bioceramics [J]. *Mater Sci Eng A*, 2004, A386: 384–389.
- [8] HONG Jin-sheng, GAO Lian. Spark plasma sintering and mechanical properties of $\text{ZrO}_2(\text{Y}_2\text{O}_3)\text{-Al}_2\text{O}_3$ composites [J]. *Materials Letters*, 2000, 43: 27–31.
- [9] GAO L, WANG H Z. $\text{SiC-ZrO}_2(3\text{Y})\text{-Al}_2\text{O}_3$ nanocomposites superfast densified by spark plasma sintering [J]. *Nanostructured Materials*, 1999, 11(1): 43–49.
- [10] KUANG X, GAROTENUTO G, NICOLAS. A review of ceramic sintering and suggestions on reducing sintering temperature [J]. *Advanced Performance Materials*, 1997, 4: 257–274.
- [11] OH D Y, KIM H C. Simultaneous synthesis and consolidation process of ultra-fine $\text{WSi}_2\text{-SiC}$ and its mechanical properties [J]. *Journal of Alloys and Compounds*, 2005, 386(Issues 1-2): 270–275.
- [12] KIM H C, OH D Y. Sintering of nanophase WC-15vol.%Co hard metals by rapid sintering process [J]. *International Journal of Refractory & Hard Materials*, 2004, 22: 197–203.
- [13] KIM H C, OH D Y. Synthesis of WC and dense WC-5vol.%Co hard materials by high-frequency induction heated combustion [J]. *Mater Sci Eng A*, 2004, A368: 10–17.
- [14] KIM H C, OH D Y. Synthesis of WC and dense WC-xvol.%Co hard materials by high-frequency induction heated combustion method [J]. *International Journal of Refractory & Hard Materials*, 2004, 22: 41–49.
- [15] ANSTIS G R, CHANTIKUL P, LAWN B R, MARSHALL D B. A critical evaluation of indentation techniques for measuring fracture toughness(I): Direct crack measurements [J]. *Journal of American Ceramic Society*, 1981, 64(9): 533–538.
- [16] PICONI C, MACCAURO G. Review, zirconia as a ceramic biomaterial [J]. *Biomaterial*, 1999, 20: 1–25.
- [17] HANNINK R H J. Transformation toughening in zirconia-containing ceramics [J]. *Journal of American Ceramic Society*, 2000, 83(3): 461–487.
- [18] BRAVO-LEON, MORIKAWA Y, KAWAHARA M, MAYO M J. Fracture toughness of nanocrystalline tetragonal zirconia with low yttria content [J]. *Acta Materialia*, 2002, 50: 4555–4562.
- [19] MISHRA R S, LESHER C E, MUKHERJEE A K. High-pressure sintering of nanocrystalline Al_2O_3 [J]. *J Am Ceram Soc*, 1996, 79: 2989–92.
- [20] ZHAN G D, KUNTZ J, WAN J, GARAY A K. Alumina-based nanocomposites consolidated by spark plasma sintering [J]. *Scripta Materialia*, 2002, 47: 737–741.

(Edited by LI Xiang-qun)